

Towards Local Visual Modeling for Image Captioning

Yiwei Ma^a, Jiayi Ji^a, Xiaoshuai Sun^{a,b}, Yiyi Zhou^a, Rongrong Ji^{a,b,c}

^a*Media Analytics and Computing Lab, Department of Artificial Intelligence, School of Informatics, Xiamen University, 361005, China*

^b*Institute of Artificial Intelligence, Xiamen University*

^c*Peng Cheng Laboratory, Shenzhen, China*

Abstract

In this paper, we study the local visual modeling with grid features for image captioning, which is critical for generating accurate and detailed captions. To achieve this target, we propose a *Locality-Sensitive Transformer Network* (LSTNet) with two novel designs, namely *Locality-Sensitive Attention* (LSA) and *Locality-Sensitive Fusion* (LSF). LSA is deployed for the intra-layer interaction in Transformer via modeling the relationship between each grid and its neighbors. It reduces the difficulty of local object recognition during captioning. LSF is used for inter-layer information fusion, which aggregates the information of different encoder layers for cross-layer semantical complementarity. With these two novel designs, the proposed LSTNet can model the local visual information of grid features to improve the captioning quality. To validate LSTNet, we conduct extensive experiments on the competitive MS-COCO benchmark. The experimental results show that LSTNet is not only capable of local visual modeling, but also outperforms a bunch of state-of-the-art captioning models on offline and online testings, *i.e.*, 134.8 CIDEr and 136.3 CIDEr, respectively. Besides, the generalization of LSTNet is also verified on the Flickr8k and Flickr30k datasets. The source code is available on GitHub: <https://github.com/xmu-xiaoma666/LSTNet>.

Keywords: Image Captioning, Attention Mechanism, Local Visual Modeling

1. Introduction

Image captioning is the task of generating a fluent sentence to describe the given image. Recent years have witnessed the rapid development of

this field, which is supported by a bunch of innovative methods [1, 2] and datasets [3, 4].

Inspired by the great success of *Bottom-up Attention* [5], most existing methods in image captioning adopt the region features extracted by the object detector as the visual representations, *e.g.*, Faster R-CNN [6]. Since the detector is pre-trained on the large-scale Visual Genome dataset [7], it can generate discriminative representations for salient regions in the image and provide complete object information for captioning. To this end, significant progress in image captioning has been made based on the region features [2, 8, 9].

However, the region features still exist obvious defects. To be specific, they are extracted from the salient regions of the image, thus often ignoring the contextual information in the background. In this case, it is inferior for the model to capture the relationship between objects. For example, as shown in Fig. 1(a), the model trained on region features fails to understand the contextual information out of the bounding boxes, thereby incorrectly describing the relationship between “woman” and “horse”. Besides, the pre-trained object detector may produce noisy, overlapped, or erroneous detections, which ultimately limits the performance upper bound of image captioning models.

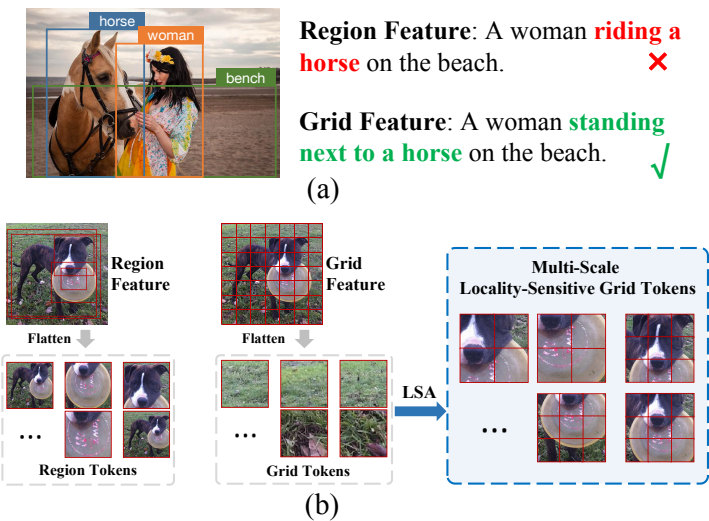


Figure 1: (a) Captions generated by Transformer with the region and grid features, respectively. (b) Region features often contain complete object information, while the grid ones are more fragmented. Our LSA is conducive to reconstructing complete object information by modeling the relationship of adjacent grids.

To compensate for the aforementioned limitations, some endeavors start to revisit the use of grid features. [10] explores grid features of the object detector to further push the performance of the visual question answering (VQA) task. RSTNet [11] and DLCT [12] first adopt grid features in Transformer-like networks, which achieve impressive performance in image captioning. However, Transformer-like architectures are not conducive to the perception of complete objects. Specifically, as shown in Fig. 1(b), a complete object may be divided into multiple adjacent grids in 2D space, while the flatten operation in Transformer inevitably destroys the local relationship of grid features. Meanwhile, recent advances [13] also show that the vanilla Transformer is less efficient in local visual modeling.

Based on the above analysis, we observe that both region and grid features have their own advantages and disadvantages. Region features contain explicit object information but lack background and relationship information. In contrast, grid features contain all information at the same time, but an object may be divided into multiple grids. As a result, the majority of the semantic information is damaged, which makes reasoning more challenging. A straightforward solution to enjoy the benefits of both features is adopting both region and grid features like DLCT [12] and GRIT [14]. However, it will lead to significantly higher computation and longer training time, because the model needs to process both features at the same time. A more efficient way is to model the local information on the grid features to compensate for the lack of object information.

Therefore, we propose a novel ***Locality-Sensitive Transformer Network (LSTNet)*** in this paper. Specifically, LSTNet strengthens local modeling to perceive object-level information from the aspects of *intra-layer interaction* and *inter-layer fusion*, respectively. For intra-layer interaction, we propose a novel multi-branch module called ***Locality-Sensitive Attention (LSA)*** to perceive fine-grained local information from different receptive fields and enhance the interactions between each grid and its neighbors. Notably, LSA can be re-parameterized into a single-branch structure during inference, thereby reducing the additional overhead of multi-scale perception. For inter-layer fusion, we design a ***Locality-Sensitive Fusion (LSF)*** module, which can align and fuse grid features from different layers for cross-layer semantical complementary. With these novel designs, LSTNet improves the ability of local visual modeling, but also greatly improves the quality of the generated captions. On the competitive MS-COCO benchmark, LSTNet presents outstanding performance on both offline and online testing, *i.e.*,

134.8 CIDEr and 136.3 CIDEr. In addition to the outstanding performance on the MS-COCO dataset, the generalization of LSTNet is also verified on the Flickr8k and Flickr30k datasets.

To sum up, our contributions are three-fold:

- To perceive object and context information with only grid features, we propose a novel LSTNet for image captioning. LSTNet not only improves the local perception ability of the model but also outperforms a bunch of recently proposed methods on the highly competitive MS-COCO benchmark.
- We propose a *Locality-Sensitive Attention (LSA)* for the intra-layer visual modeling in Transformer, which is a re-parameterized module for enhancing the interaction between each grid feature and its local neighbors.
- We propose a *Locality-Sensitive Fusion (LSF)* to aggregate inter-layer object semantic information for image captioning, which is conducive to inter-layer semantic understanding.

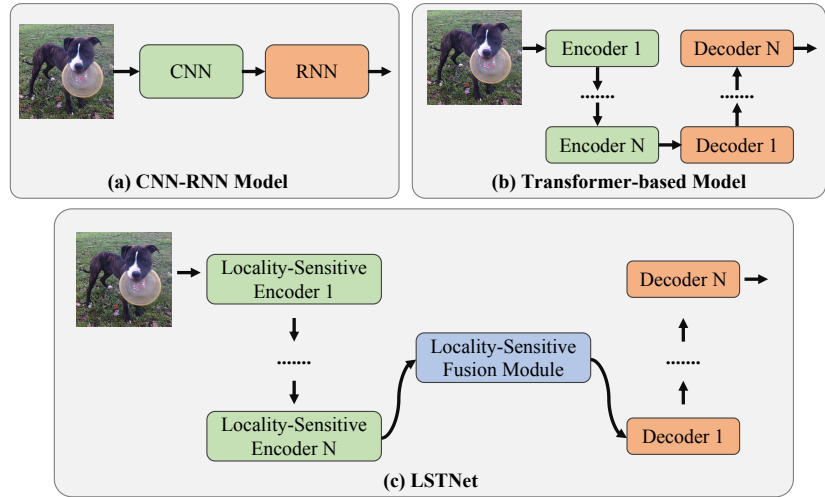


Figure 2: Illustration of CNN-RNN model (a), Transformer-based model (b), and LSTNet (c) for image captioning.

2. Related Work

2.1. Image Captioning

Image captioning is a challenging task, and enormous effort has been made to solve this problem. With years of development, a great improvement can be observed with a flurry of methods [5, 8, 11, 15–18]. The existing image captioning methods can be roughly divided into two categories: 1) the CNN-RNN model, 2) the Transformer-based model. As shown in Fig. 2(a), the CNN-RNN model uses CNN to encode images into vectorial representations and then adopts an RNN-based decoder to fuse these vectorial representations to provide content-related descriptions for input images. Specifically, [15] uses Convolutional Neural Network (CNN) to encode images and adopts Long Short-Term Memory (LSTM) as a decoder to generate captions. [16] exploits the adaptive attention mechanism to decide whether to attend to visual or non-visual information at each time step. [5] uses the pre-trained Fast R-CNN [6] to extract salient objects as regional visual features, which is conducive to generating accurate captions. With the development of Transformer [19], a lot of researchers are investigating the application of Transformer-based models on the image captioning task, which is illustrated in Fig. 2(b). [8] introduces Bi-linear Pooling into the Transformer model to capture 2^{nd} order interactions. [11] proposes to adaptively measure the contribution of visual and language cues on the top of the transformer decoder before word prediction. [12] presented a Dual-level Collaborative Transformer (DLCT) to accomplish the complementarity of the region and grid features. To improve the semantic understanding ability of Transformer, [18] proposes a Transformer-based captioning model with both spatial and channel-wise attention. [20] proposes a Geometry Attention Transformer (GAT) model to further leverage geometric information in image captioning. To consider the visual persistence of object features, [21] introduces a VP-Net via inserting visual persistence modules in both the encoder and decoder. [22] proposes a novel CtxAdpAtt model, which adopts the linguistic context to explore related visual relationships between different objects effectively. To alleviate the disadvantages of using GCN-based encoders to represent the relation information among scene graphs, ReFormer[23] explores a novel architecture to explicitly express the relationship between objects in the image.

Our LSTNet is in line with the Transformer-base approach. However, when processing grid features, the Transformer ignores visual locality, which is important for identifying objects in the image. As shown in Fig. 2(c),

we propose the Locality-Sensitive Attention (LSA) module and Locality-Sensitive Attention (LSA) module to enhance local visual modeling.

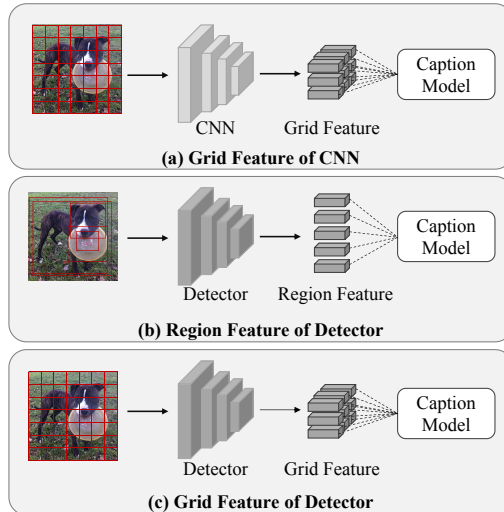


Figure 3: Three main stages of visual features used in the image captioning task: **(a)** Grid features extracted by CNN, *e.g.*, ResNet [24]; **(b)** Region features extracted by the pre-trained detector, *e.g.*, Faster R-CNN [6], which requires time-consuming post-processing operations, *e.g.*, NMS [25]; **(c)** Grid features extracted from the feature map of CNN in the object detector.

2.2. Region features & Grid features

The visual features used in image captioning go through three main stages: Grid \rightarrow Region \rightarrow Grid. In the first grid stage, some pioneering works [16, 26, 27] adopt grid visual features extracted from CNN [24] to represent images, which is illustrated in Fig. 3(a). For example, [26] first propose the image captioning task, and adopt CNN to encode visual features and RNN to decode the caption. To capture the importance of different grids in an image, [27] applies the attention mechanism to the visual features before decoding the caption. [16] propose adaptive attention on the visual feature, which is extracted from the last convolutional layer of ResNet101 [24]. As shown in Fig. 3(b), to obtain foreground information, [5] adopts an object detector [6] pre-trained on VG [7] to extract region features, which are widely used in a lot of multi-modal tasks [2, 28]. As shown in Fig. 3(c), to compensate for the defects (*e.g.*, time-consuming) of region features, [10] revisits the grid

feature in the object detector, and finds that it could achieve competitive performance in VQA, the effectiveness of which has also been validated in image captioning [11, 12].

Compared with previous methods [2, 8, 9] based on region features, our proposed LSTNet based on grid features can capture the contextual information out of bounding boxes, thus generating more accurate captions. On the other hand, compared with existing methods [11] based on grid features, our proposed LSTNet considers the locality of the grid features and models the relationship of neighboring grids, which is conducive to recognizing the objects in the image. DLCT [12] adopts bounding boxes to assist grid features to locate objects. However, due to the adoption of both grid and region features, the model needs to bear more training and prediction overhead, *e.g.*, LSTNet runs over three times faster than DLCT in the cross-entropy training stage, whose performance is severely limited by the accuracy of bounding boxes. Our proposed LSTNet captures intra- and inter-layer local relationships, leading to more detailed and finer-grained grid features for image captioning.

2.3. Multi-head Self-Attention in Transformer

Transformer is originally proposed to solve natural language processing (NLP) tasks. Due to its powerful modeling ability, the transformer has also been widely used in computer vision (CV) and multi-modal tasks in recent years. The key component of the transformer is the multi-head self-attention (MSA) module, which can effectively model the relationship and context of the input at different positions. Specifically, a h -head self-attention is formulated as:

$$\text{MultiHead}(\mathbf{Q}, \mathbf{K}, \mathbf{V}) = \text{Concat}(\text{head}_1, \text{head}_2, \dots, \text{head}_h) \mathbf{W}^O, \quad (1)$$

where $\mathbf{Q}, \mathbf{K}, \mathbf{V} \in \mathbb{R}^{N \times d}$ represent the input query, key, and value, respectively. N is the length of input, d is the hidden dimension in each head. $\mathbf{W}^O \in \mathbb{R}^{hd \times d}$ is a learnable matrix for the output of all heads. For each head, the attention is formulated as follows:

$$\text{head}_i = \text{Attention} \left(\mathbf{Q}_i^Q, \mathbf{K} \mathbf{W}_i^K, \mathbf{V} \mathbf{W}_i^V \right) = \text{softmax} \left(\frac{\mathbf{Q} \mathbf{W}_i^Q (\mathbf{K} \mathbf{W}_i^K)^T}{\sqrt{d}} \right) \mathbf{V} \mathbf{W}_i^V, \quad (2)$$

where $\mathbf{W}_i^Q, \mathbf{W}_i^K, \mathbf{W}_i^V \in \mathbb{R}^{d \times d}$ are the learnable matrices for input query, key, and value, respectively.

3. Approach

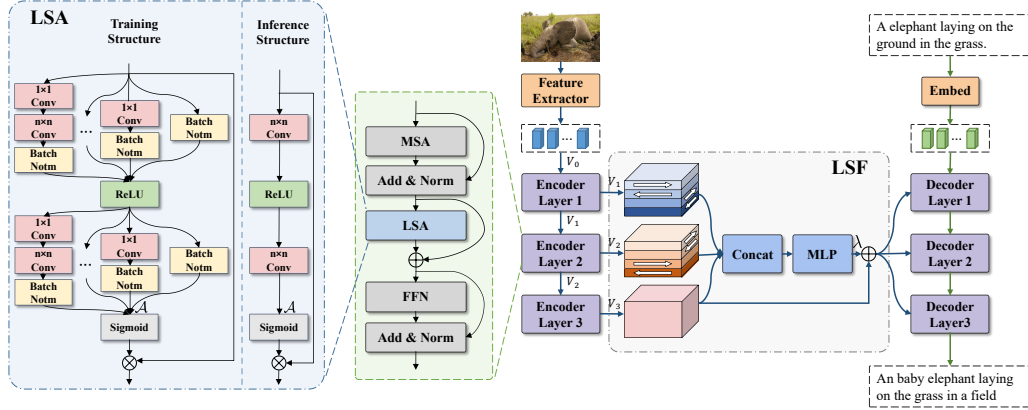


Figure 4: Overview of our proposed LSTNet. Grid features are used as visual representations and fed to the visual encoder. Locality-Sensitive Attention (LSA) is inserted after self-attention to capture local dependencies. We also apply reparameterization technology to reduce its overhead during inference. The output of encoding layers is further processed by Locality-Sensitive Fusion (LSF) to achieve cross-layer aggregation, which can also provide the semantics of different layers for local visual modeling. MSA and FFN represent Multi-head Self-Attention and Feed-Forward Networks, respectively.

3.1. Overview

As shown in Fig. 4, our proposed *Locality-Sensitive Transformer Network (LSTNet)* follows the encoder-decoder paradigm. Concretely, the encoder takes the visual features as input and then models their relationships by the encoder layers, where *Locality-Sensitive Attention (LSA)* module is adopted to enhance local visual modeling. Then, *Locality-Sensitive Fusion (LSF)* aggregates the visual features from different encoding layers, based on which the decoder predicts caption words to describe the given visual content.

The visual features before the l -th encoder layer are denoted as $V_{l-1} \in \mathbb{R}^{N_v \times c}$ ($N_v = h \times w$), where h, w, c represent the height, width and channel dimension of visual features, respectively.

Each encoder layer of LSTNet consists of three components: (1) a Multi-head Self-Attention (MSA) module; (2) a Locality-Sensitive Attention (LSA) module; (3) a Feed-Forward Network (FFN). The visual features V_{l-1} from the last encoder layer is first processed by the MSA as follows (LayerNorm operation is omitted for conciseness):

$$V'_{l-1} = V_{l-1} + MSA(V_{l-1}, V_{l-1}, V_{l-1}), \quad (3)$$

where $MSA(\cdot)$ is the standard Multi-head Self-Attention in Transformer [19]. Because MSA can model the relationship and context of any two positions in the input sequence, MSA is conducive to capturing long-range dependencies and modeling global information among grids.

Self-Attention is often inefficient in capturing the local details, which, however, is critical for grid visual features as explained in Sec.1. Thus, based on V'_{l-1} , LSA is adopted to capture the dependencies of neighboring grids to further refine visual features:

$$V''_{l-1} = V'_{l-1} + LSA(V'_{l-1}), \quad (4)$$

where the detail of LSA is described in the next subsection. Because LSA is composed of cascaded convolution layers, which can model the relationship between adjacent grids, LSA is conducive to modeling local relationships among grids.

Then the output of the LSA module is fed to FFN for the interaction in the channel domain:

$$V_l = V''_{l-1} + FFN(V''_{l-1}), \quad (5)$$

$$FFN(x) = \max(0, xW_1 + b_1)W_2 + b_2. \quad (6)$$

Different from previous Transformer-based models, which only feed the output of the top encoder layer to the decoder, our proposed LSF module aggregates visual features from all encoder layers to obtain richer features in semantic by Locality-Sensitive Fusion (LSF):

$$V^* = LSF(V_1, V_2, \dots, V_n), \quad (7)$$

where n is the number of encoder layers.

Finally, V^* is fed into the decoder to generate the captions, which is the same as that of the vanilla Transformer [19].

3.2. Locality-Sensitive Attention (LSA)

As visualized in Fig. 1(b), an object in the image may be divided into several fragments and distributed in various grids, which destroys the spatial and semantic information of visual objects. A reasonable approach is to strengthen the interaction of local information, which is also in line with the assumption that features close to each other in vision are more likely to be correlated.

Thus, to capture the local details and model the interaction between adjacent grids, we propose a multi-scale locality-sensitive module, namely Locality-Sensitive Attention (LSA). Specifically, the output feature $V' \in \mathbb{R}^{N \times C}$ of the MSA module is a grid sequence, where N is the number of grids, C is the size of channel dimension. We first reshape $V' \in \mathbb{R}^{N \times C}$ to $V' \in \mathbb{R}^{H \times W \times C}$, where H, W are the height and width of the grid feature. Then, we use two multi-scale 2D CNNs in series with an activation function (*i.e.*, ReLU) in between to obtain the visual features \mathcal{A} after multi-scale local perception, which could be formulated as follows:

$$\mathcal{A} = MSC_2(\sigma(MSC_1(V'))), \quad (8)$$

where $\sigma(\cdot)$ is the activation function and $MSC_i(\cdot)$ represents a multi-scale CNN implemented by multi-branch CNNs:

$$MSC_i(x) = BN_1^i(F_1^i(x)) + \dots + BN_N^i(F_N^i(x)), \quad (9)$$

where $i \in \{1, 2\}$, N is the number of branches, $BN_j(\cdot)$ is Batch Normalization [29], $F_j(\cdot)$ represents identity mapping, one convolution module, or several convolution modules in series, and $j \in \{1, \dots, N\}$. In our LSTNet, the number of branches N is 3. As shown in the blue area in Fig. 4, three branches are (1) the identity mapping, (2) the 1×1 Conv, and (3) the sequential combination of 1×1 Conv and 3×3 Conv, respectively.

During inference, the multi-branch structure $MSC_i(\cdot)$ can be simplified into a single-branch structure to save the number of parameters and computational cost by using some structural reparameterization techniques [30, 31] without any performance loss:

$$MSC_i(x) \rightarrow F^i(x), \quad (10)$$

where $F^i(x)$ is a 3×3 convolution, and $i \in \{1, 2\}$.

To get the attention weight for each grid, we also apply the Sigmoid function to \mathcal{A} . Finally, we reweight the output feature of Self-Attention layer V' according to locality-sensitive attention map as follows:

$$V'' = V' \otimes \text{Sigmoid}(\mathcal{A}), \quad (11)$$

where \otimes represents element-wise multiplication.

3.3. Locality-Sensitive Fusion (LSF)

Features from different layers tend to contain semantic information of various levels [2]. However, most existing image captioning methods only feed the feature of the top encoder layer to the decoder, leading to low-level information loss. To avoid such information loss, we fuse the features of all layers in the encoder and then feed the fused feature into the decoder.

Technically, we introduce a simple *Spatial Shift* operation to enable each grid to align with its neighbor grids, and then the Multi-Layer Perceptron (MLP) is used to interact not only in the channel domain but also in the spatial domain.

Particularly, denoting features from the l -th encoder layer as $V_l \in \mathbb{R}^{h \times w \times c}$ (the reshape operation is omitted here), V_1 and V_2 are shifted by different Spatial Shift operations (*i.e.*, $SS_1(\cdot)$ and $SS_2(\cdot)$), which can be represented as Eq. 12 and Eq. 13:

$$\begin{aligned} V_1[d_s : h, :, 0 : c/4] &= V_1[0 : h - d_s, :, 0 : c/4], \\ V_1[0 : h - d_s, :, c/4 : c/2] &= V_1[d_s : h, :, c/4 : c/2], \\ V_1[:, d_s : w, c/2 : 3c/4] &= V_1[:, 0 : w - d_s, c/2 : 3c/4], \\ V_1[:, 0 : w - d_s, 3c/4 : c] &= V_1[:, d_s : w, 3c/4 : c], \end{aligned} \quad (12)$$

$$\begin{aligned} V_2[:, d_s : w, 0 : c/4] &= V_2[:, 0 : w - d_s, 0 : c/4], \\ V_2[:, 0 : w - d_s, c/4 : c/2] &= V_2[:, d_s : w, c/4 : c/2], \\ V_2[d_s : h, :, c/2 : 3c/4] &= V_2[0 : h - d_s, :, c/2 : 3c/4], \\ V_2[0 : h - d_s, :, 3c/4 : c] &= V_2[d_s : h, :, 3c/4 : c], \end{aligned} \quad (13)$$

where V_i is the output feature of the i -th encoder layer, d_s is the shift distance of Spatial Shift, which determines the scope of local interaction. The output of the top encoder layer V_3 is not processed by any shift operations. The illustration of Spatial Shift can be observed in Fig. 4 and Fig. 5.

Then, shifted features from different layers are concatenated together:

$$V_c = \text{Concat}(V_1, V_2, V_3). \quad (14)$$

Table 1: Leaderboard of the published state-of-the-art image captioning models on the COCO online testing server.

Model	BLEU-1		BLEU-2		BLEU-3		BLEU-4		METEOR		ROUGE-L		CIDEr-D	
	c5	c40	c5	c40										
SCST [32] <small>cvpr'17</small>	78.1	93.7	61.9	86.0	47.0	75.9	35.2	64.5	27.0	35.5	56.3	70.7	114.7	116.0
LSTM-A [33] <small>iccv'17</small>	78.7	93.7	62.7	86.7	47.6	76.5	35.6	65.2	27.0	35.4	56.4	70.5	116.0	118.0
Up-Down [5] <small>cvpr'18</small>	80.2	95.2	64.1	88.8	49.1	79.4	36.9	68.5	27.6	36.7	57.1	72.4	117.9	120.5
RFNet [34] <small>eccv'18</small>	80.4	95.0	64.9	89.3	50.1	80.1	38.0	69.2	28.2	37.2	58.2	73.1	122.9	125.1
GCN-LSTM [35] <small>eccv'18</small>	80.8	95.2	65.5	89.3	50.8	80.3	38.7	69.7	28.5	37.6	58.5	73.4	125.3	126.5
SGAE [36] <small>cvpr'19</small>	81.0	95.3	65.6	89.5	50.7	80.4	38.5	69.7	28.2	37.2	58.6	73.6	123.8	126.5
AgANet [9] <small>cvpr'19</small>	81.0	95.0	65.8	89.6	51.4	81.3	39.4	71.2	29.1	38.5	58.9	74.5	126.9	129.6
CAVPN [37] <small>TPAMI'19</small>	80.1	94.9	64.7	88.8	50.0	79.7	37.9	69.0	28.1	37.0	58.2	73.1	121.6	123.8
ETA [38] <small>iccv'19</small>	81.2	95.0	65.5	89.0	50.9	80.4	38.9	70.2	28.6	38.0	58.6	73.9	122.1	124.4
M^2 Transformer [2] <small>cvpr'20</small>	81.6	96.0	66.4	90.8	51.8	82.7	39.7	72.8	29.4	39.0	59.2	74.8	129.3	132.1
XTransformer (ResNet-101) [8] <small>cvpr'20</small>	81.3	95.4	66.3	90.0	51.9	81.7	39.9	71.8	29.5	39.0	59.3	74.9	129.3	131.4
XTransformer (SENet-154) [8] <small>cvpr'20</small>	81.9	95.7	66.9	90.5	52.4	82.5	40.3	72.4	29.6	39.2	59.5	75.0	131.1	133.5
DLCT (ResNeXt101) [12] <small>aaai'21</small>	82.0	96.2	66.9	91.0	52.3	83.0	40.2	73.2	29.5	39.1	59.4	74.8	131.0	133.4
DLCT (ResNeXt152) [12] <small>aaai'21</small>	82.4	96.6	67.4	91.7	52.8	83.8	40.6	74.0	29.8	39.6	59.8	75.3	133.3	135.4
RSTNet(ResNext101) [11] <small>cvpr'21</small>	81.7	96.2	66.5	90.9	51.8	82.7	39.7	72.5	29.3	38.7	59.2	74.2	130.1	132.4
RSTNet(ResNext152) [11] <small>cvpr'21</small>	82.1	96.4	67.0	91.3	52.2	83.0	40.0	73.1	29.6	39.1	59.5	74.6	131.9	134.0
GAT [20] <small>expert syst. appl.'22</small>	81.1	95.1	66.1	89.7	51.8	81.5	39.9	71.4	29.1	38.4	59.1	74.4	127.8	129.8
VPNet [21] <small>neurocomputing'22</small>	81.4	95.5	66.4	90.3	52.0	82.1	40.0	72.1	29.3	38.9	59.3	74.9	128.2	130.6
CtxAdpAtt [22] <small>tmm'22</small>	81.0	95.2	65.5	91.0	51.5	81.7	39.3	70.9	29.4	39.0	59.6	75.1	128.5	131.0
ReFormer [23] <small>mm'22</small>	82.0	96.7	-	-	-	-	40.1	73.2	29.8	39.5	59.9	75.2	129.9	132.8
LSTNet (ResNeXt-101)	82.2	96.2	67.2	91.2	52.7	83.5	40.6	73.8	29.6	39.3	59.6	75.0	132.0	134.5
LSTNet (ResNeXt-152)	82.6	96.7	67.8	92.0	53.3	84.3	41.1	74.7	29.9	39.6	60.0	75.4	134.0	136.3

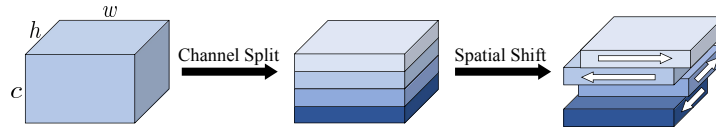


Figure 5: Illustration of the *Spatial Shift* operation. c, h, w are the size of the channel, height, and width dimension, respectively.

Theoretically, MLP can’t model the relationships among adjacent grids. However, after being shifted by the Spatial Shift operation, which aligns each grid with its neighbors, MLP can communicate in both channel and spatial domains:

$$\tilde{V} = \sigma(V_c W_1) W_2, \quad (15)$$

where $\sigma(\cdot)$ is the ReLU activation function, $W_1 \in \mathbb{R}^{3c \times 3c}$ and $W_2 \in \mathbb{R}^{3c \times c}$ are the learnable projection matrices.

To further enhance the descriptive power of visual features, we combine the outputs of the top encoder layer with the fused feature \tilde{V} via a residual connection:

$$V^* = \lambda \tilde{V} + V_{top}, \quad (16)$$

where V_{top} is the feature of the top encoder layer, $V_{top} = V_3$ in our LSTNet, and λ serves as a weighting factor.

Table 2: Comparisons with SOTAs on the Karpathy test split. All values are reported as percentages (%), where B-N, M, R, and C are short for BLEU-N, METEOR, ROUGE-L, and CIDEr scores.

Model	B-1	B-4	M	R	C	S
SCST [32] <small>cvpr'17</small>	-	34.2	26.7	55.7	114.0	-
Up-Down [5] <small>cvpr'18</small>	79.8	36.3	27.7	56.9	120.1	21.4
RFNet [34] <small>eccv'18</small>	79.1	36.5	27.7	57.3	121.9	21.2
GCN-LSTM [35] <small>eccv'18</small>	80.5	38.2	28.5	58.3	127.6	22.0
SGAE [36] <small>cvpr'19</small>	80.8	38.4	28.4	58.6	127.8	22.1
CAVPN [37] <small>tpami'19</small>	-	38.6	28.3	58.5	126.3	21.6
AoANet [9] <small>cvpr'19</small>	80.2	38.9	29.2	58.8	129.8	22.4
ORT [39] <small>neurips'19</small>	80.5	38.6	28.7	58.4	128.3	22.6
Transformer [19] <small>neurips'17</small>	80.7	38.6	29.1	58.5	130.1	22.7
M^2 Transformer [2] <small>cvpr'20</small>	80.8	39.1	29.2	58.6	131.2	22.6
XTransformer [8] <small>cvpr'20</small>	80.9	39.7	29.5	59.1	132.8	23.4
DLCT [12] <small>aaai'21</small>	81.4	39.8	29.5	59.1	133.8	23.0
RSTNet [11] <small>cvpr'21</small>	81.1	39.3	29.4	58.8	133.3	23.0
GAT [20] <small>expert syst. appl.'22</small>	80.8	39.7	29.1	59.0	130.5	22.9
VPNet [21] <small>neurocomputing'22</small>	80.9	39.7	29.3	59.2	130.4	23.2
CtxAdpAtt [22] <small>tmm'22</small>	80.5	39.1	29.3	59.3	130.1	23.6
ReFormer [23] <small>mm'22</small>	-	39.8	29.7	59.8	131.2	23.0
LSTNet	81.5	40.3	29.6	59.4	134.8	23.1

Specifically, the motivation for LSF comes from two aspects: 1) The output feature map of different encoder layers has different semantics (*i.e.*, the high-level feature map has high-level semantic information, and the low-level feature map has low-level semantic information). The traditional Transformer only feeds the feature map of the last layer in the encoder into the decoder, ignoring the low-level semantic information. LSF solves this problem by fusing the outputs of all encoder layers, considering both high-level and low-level semantic information. 2) The LSF module can interact with local grids through spatial shift operation, which is conducive to modeling object-level information.

3.4. Objectives

Given the ground-truth caption $y_{1:T}^*$ and the captioning model with parameters θ , where T is the length of the caption, we pre-train the model

using Cross-Entropy (CE) loss as follows:

$$L_{CE} = - \sum_{t=1}^T \log (p_{\theta}(y_t^* | y_{1:t-1}^*)). \quad (17)$$

Then we further optimize the model using CIDEr and BLEU-4 scores by Self-Critical Sequence Training (SCST) [32] as follows:

$$\nabla_{\theta} L_{RL}(\theta) = -\frac{1}{k} \sum_{i=1}^k (r(y_{1:T}^i) - b) \nabla_{\theta} \log p_{\theta}(y_{1:T}^i), \quad (18)$$

where k is the beam size, $r(\cdot)$ is the sum of CIDEr and BLEU-4, and $b = (\sum_i r(y_{1:T}^i)) / k$ is the reward baseline.

4. Experiment

4.1. Datasets

We conduct our experiments on the popular MS-COCO [3] image captioning dataset. It contains 123,287 images, including 82,783 training images, 40,504 validation images, and 40,775 testing images, each of which is annotated with 5 captions. We adopt the split provided by [40] for the offline test, where 5,000 images are used for validation, 5,000 images for testing, and the rest images for training. Besides, we also upload generated captions of the official testing set for online evaluation ¹.

4.2. Implementation Details

The grid features are extracted from a pre-trained Faster-RCNN [6] provided by [10], where a stride-1 C_5 backbone and 1×1 RoIPool with two FC layers are used as the detection head for training Faster R-CNN on the VG dataset. Specifically, we adopt the C_5 feature maps and average-pool them as 7×7 spatial size. Note that we do not use any extra data preprocessing, except simple augmentations (*e.g.*, RandomCrop, RandomRotation). The d_{model} in the LSTNet is 512, the expansion rate in the FFN is 4, the number of heads is 8, and the size of the beam search is 5.

We use Adam optimizer to train our model in both stages and adopt the relative position encoding following [12]. In the CE training stage, the batch

¹<https://competitions.codalab.org/competitions/3221#results>

size is 50, and the learning rate is linearly increased to 1×10^{-4} during the first 4 epochs. Afterwards, we set it to 2×10^{-5} , 4×10^{-6} at 10-th and 12-th epoch. After 18 epochs of CE pre-training, we optimize the model by SCST with the batch size of 100 and learning rate of 5×10^{-6} . The learning rate will be set to 2.5×10^{-6} , 5×10^{-7} , 2.5×10^{-7} , 5×10^{-8} at the 35-th, 40-th, 45-th, 50-th epoch, and the SCST training will last 42 epochs.

4.3. Performance Comparison

In this section, we compare our LSTNet with SOTAs on both offline and online evaluations. The compared models include: SCST [32], Up-Down [5], RFNet [34], GCN-LSTM [35], SGAE [36], AoANet [9], ETA [38], ORT [39], Transformer [19], M^2 Transformer [2], XTransformer [8], RSTNet [11] and DLCT [12]. Following the standard evaluation criterion, we adopt BLEU-N [41], METEOR [42], ROUGE-L [43], CIDEr [44], SPICE [45] to evaluate the performance.

4.3.1. Online Evaluation

Tab. 1 shows the performance comparisons of LSTNet and other SOTA methods on the online COCO test server with 5 reference captions (c5) and 40 reference captions (c40). For fair comparisons, we also use the ensemble of four models following [2] and adopt two common backbones (*i.e.*, ResNeXt-101, ResNeXt-152 [46]). Notably, our LSTNet outperforms other SOTA methods in all metrics by significant margins. Surprisingly, we observe that *LSTNet with ResNeXt-101* performs better than *RSTNet with ResNeXt-152* and *X-Transformer with SENet-154* on most metrics.

4.3.2. Offline Evaluation

Tab. 2 summarizes the performance of the state-of-the-art models and our approach to the offline COCO Karpathy test split. Note that for fair comparisons, we report the results of single models without using any ensemble technologies. We can observe that our proposed LSTNet outperforms all the other SOTA models in terms of most metrics. Notably, the CIDEr score of our LSTNet achieves **134.8%**, outperforming the strongest competitor DLCT by **1.0%**, which adopts both region and grid features.

We observe that the LSTNet with the grid feature performs better than some models (*e.g.*, M^2 Transformer [2], XTransformer [8]) with region features. We think the reasons why the grid-level scheme in our paper performs better than the object-level scheme are as follows: 1) The region feature’s

Table 3: Comparisons with SOTA methods on the Karpathy test split using the same ResNeXt101 [46] grid feature.

Model	B-1	B-4	M	R	C	S
Up-Down [5] <small>cvpr'18</small>	75.0	37.3	28.1	57.9	123.8	21.6
AoANet [9] <small>cvpr'19</small>	80.8	39.1	29.1	59.1	130.3	22.7
Transformer [19] <small>neurips'17</small>	81.0	38.9	29.0	58.4	131.3	22.6
M^2 Transformer <small>cvpr'20 [2]</small>	80.8	38.9	29.1	58.5	131.8	22.7
XTransformer [8] <small>cvpr'20</small>	81.0	39.7	29.4	58.9	132.5	23.1
DLCT [12] <small>aaai'21</small>	81.4	39.8	29.5	59.1	133.8	23.0
RSTNet [11] <small>cvpr'21</small>	81.1	39.3	29.4	58.8	133.3	23.0
LSTNet	81.5	40.3	29.6	59.4	134.8	23.1

background information is missing, and the grid feature extracts all of the information in the image. Specifically, visual region features are collected from the image’s salient parts, typically omitting contextual information. Because of the lack of background information, the model performs poorly in capturing relationships between objects. The grid feature, on the other hand, collects all spatial information from the image. 2) The pre-trained object detector often involves noisy, overlapped, or erroneous detections, which ultimately limits the performance upper bound of image captioning models. On the other hand, grid features do not provide detection information, so the impact of error detection is avoided. 3) In grid features, an object is divided into different grids, and this is the motivation of this paper. Our approach enables the model to capture local information and solves this problem.

4.3.3. Fair Comparisons with SOTA Methods

To eliminate the interference of different visual features, we conduct experiments on the same grid features to compare the LSTNet and other SOTA methods. As reported in Tab. 3, compared with other methods on the same visual features, our proposed LSTNet still achieves superior performance on all metrics.

4.4. Ablation Study

4.4.1. Effect of Different Branches of LSA

To validate the impact of each branch, we conduct a series of experiments by leveraging different branches of LSA. The performance of LSA with different branches is illustrated in Tab. 4. By analyzing this table, we gain the following observations:

- Compared with the model without LSA (line 1), adopting LSA (line 2-7) with either one or more branches is helpful to generate better captions. Moreover, the more branches are adopted, the better performance tends to be achieved. This may be because the proposed LSA module improves the local perception ability of the model, so it is beneficial to the perception of object information.
- As shown in Tab. 4, equipping one branch (lines 2,3,4) outperforms the model with 0 branches (line 1) on most evaluation metrics. By comparing the model with one branch (lines 2,3,4) to the model with two branches (lines 5,6,7), we can see that the model with two branches outperforms the model with one branch on most metrics, particularly CIDEr. Furthermore, we can see that the completed LSTNet (line 8) with all three branches performs the best. This may be attributed to that objects in the image vary in size, so more branches are conducive to strengthening the multi-scale modeling ability for objects of different sizes. Importantly, by using reparameterization techniques, more branches of LSA will not lead to higher overhead during inference.

4.4.2. Effect of Different Arrangements of LSA and SA

To explore the impact of various arrangements of Locality-Sensitive Attention (LSA) and Self-Attention (SA), we compare three methods to combine LSA and SA: (1) sequential LSA-SA, (2) sequential SA-LSA, (3) parallel usage of SA and LSA. As shown in Tab. 5, we can observe that the performance of the sequential SA-LSA is better than the others. The main reason may be that the features processed by SA are coarse-grained, and our proposed LSA, which aims to model local relationships, is helpful to further refine the visual features.

4.4.3. Effect of Different Shift Distances of LSF

To explore the impact of shift distance d_s of LSF, we conduct experiments by increasing d_s from 0 to 4 ($d_s = 0$ means that all features are not shifted). From Tab. 6, we could observe that shifted LSF performs better than the unshifted one. This can be attributed to that shifted LSF makes each grid can interact with neighboring grids during fusing, thus enhancing the local modeling. However, when the shift distance is greater than 1, the performance begins to drop and $d_s = 1$ performs best. The reason may be

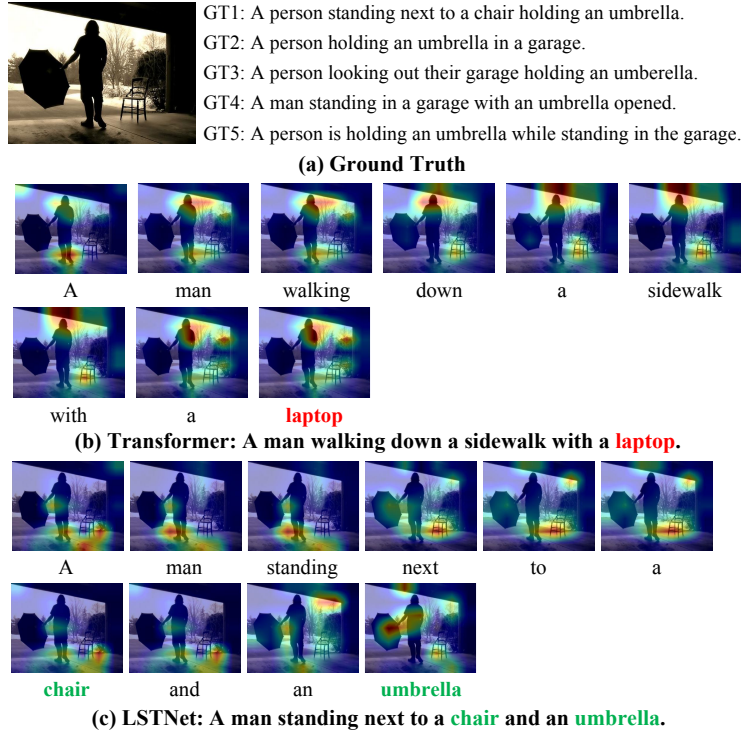


Figure 6: The ground truth (a) and the visualization of attended images along with the caption generation of standard Transformer (b) and LSTNet (c). The most significant difference between the two generated captions is highlighted in bold.

that the large shift promotes the long-distance interaction, but ignores local modeling.

4.4.4. Effect of λ in LSA

To choose the best weighting factor λ in Eq. 16, we also conduct a group of experiments. From Tab. 7, we could find that too large λ will lead to performance degradation, and $\lambda = 0.2$ performs well on most metrics. Thus, we use $\lambda = 0.2$ for our experiments if not specified.

4.4.5. Effect of Decoupling LSA and LSF

To gain insights into the proposed LSA and LSF modules, we decouple these two modules in the experiment. As reported in Tab. 8, compared with the complete model, the performance of the model without LSA+LSF

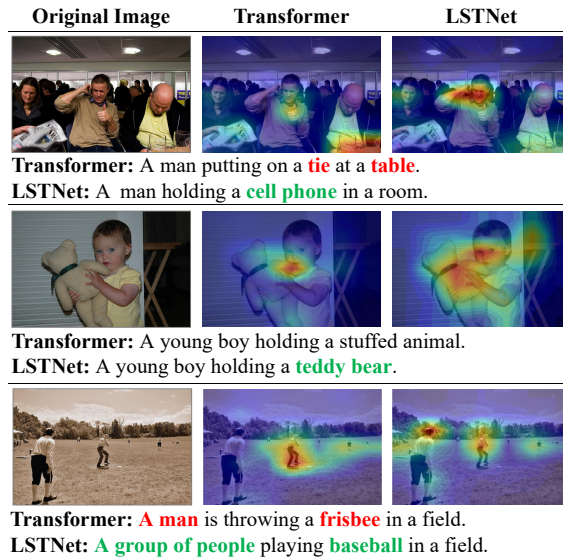


Figure 7: Some examples of captions generated by Transformer and LSTNet on the same grid features and comparisons of corresponding attention map of the top encoder layer of Transformer and LSTNet.

degrades dramatically. Particularly, it drops absolutely by **1.4%** and **3.5%** on BLEU-4 and CIDEr respectively, which demonstrates the vital importance of LSA and LSF. Particularly, our LSA and LSF achieve performance gains of 2.3% and 2.4% on the CIDEr score, respectively. This shows that LSA and LSF modules can promote each other to achieve better performance.

4.4.6. Effect of Different Approaches to Fuse Features

To justify the effectiveness of LSF, we design a group of experiments by replacing LSF with various modules to fuse features. As shown in Tab. 9, we can find that fusing features from different layers improves the performance when compared with the results in the first row (*i.e.*, without fusing features). The main reason may be that features from different layers are complementary in semantic information and fusing features will enrich visual features. Moreover, our proposed LFS module outperforms other modules by a large margin, which strongly illustrates the validity of LFS.

4.4.7. Effect of Different Grid Sizes

To explore the impact of different grid sizes, we conduct a series of experiments by setting the visual features to different sizes via average pooling. As

Table 4: Ablation studies on various branches. All branches contain BatchNorm, and all models are not equipped with LSF. All values are reported as percentages (%), B-N, M, R, C, and S are short for BLEU-N, METEOR, ROUGE-L, CIDEr, and SPICE scores.

Identity	1×1	1×1+3×3	B-1	B-4	M	R	C	S
×	×	×	81.0	38.9	29.0	58.4	131.3	22.6
✓	×	×	81.1	38.9	29.1	58.4	131.6	22.6
×	✓	×	81.1	39.2	29.2	58.9	132.2	22.7
×	×	✓	81.2	39.4	29.2	58.9	132.3	22.7
✓	✓	×	81.2	39.6	29.1	59.0	133.5	22.7
✓	×	✓	81.2	39.6	29.2	58.9	133.4	22.6
×	✓	✓	81.2	39.6	29.3	59.1	133.5	22.8
✓	✓	✓	81.2	39.7	29.3	59.1	133.6	22.8

Table 5: Ablation studies on various arrangements of SA and LSA. + is sequential connection, & represents parallel connection.

Arrangement	B-1	B-4	M	R	C	S
LSA + SA	81.1	39.6	29.1	59.0	133.4	22.8
SA + LSA	81.2	39.7	29.3	59.1	133.6	22.8
SA & LSA	81.0	39.5	28.9	59.0	132.7	22.7

shown in Tab. 10, the performance of image captioning gradually improves as the grid size is increased. This is explained by the fact that a larger image feature offers more fine-grained and richer semantic information, and the image captioning model will produce more accurate descriptions as a result of these details.

4.5. Quantitative Analysis

By comparing conventional metrics (*e.g.*, BLEU-N, CIDEr, SPICE), it is difficult to determine whether our method significantly improves the performance of image captioning. Aiming to demonstrate the efficacy and superiority of our proposed LSTNet in an intuitive way, we conduct a two-tailed t-test with paired samples to compare LSTNet with a standard Transformer. To be specific, we first perform the two-tailed t-test for each conventional metric to explore whether the quality of caption generated by LSTNet is significantly improved compared with the standard Transformer. Besides, we also report the semantic subcategories of SPICE scores (*i.e.*, Relation, Cardinality, Attribute, Size, Color, and Object), which can be used to measure

Table 6: Ablation studies on various shift distances of LSF. All models are equipped with both LSA and LSF modules.

Shift Distance	B-1	B-4	M	R	C	S
$d_s = 0$	81.2	39.9	29.3	59.1	133.9	22.8
$d_s = 1$	81.5	40.3	29.6	59.4	134.8	23.1
$d_s = 2$	81.4	40.1	29.5	59.2	134.4	22.9
$d_s = 3$	81.3	40.1	29.5	59.2	134.2	22.8
$d_s = 4$	81.3	40.0	29.4	59.1	134.0	22.8

Table 7: Performance comparisons with different weight factors λ . All models are equipped with both LSA and LSF modules.

λ	B-1	B-4	M	R	C	S
$\lambda = 0.1$	81.7	40.3	29.4	59.3	134.3	22.9
$\lambda = 0.2$	81.5	40.3	29.6	59.4	134.8	23.1
$\lambda = 0.3$	81.6	40.2	29.5	59.3	134.5	23.0
$\lambda = 0.5$	81.6	40.3	29.5	59.3	134.5	30.0
$\lambda = 0.7$	81.4	40.0	29.4	59.0	134.0	22.9

the semantic relevance between generated sentences and ground truth. Furthermore, for each comprehensive SPICE score, we do a detailed two-tailed t-test with matched data to see if these semantic indicators have also been significantly improved.

The conventional metrics and corresponding p-values for the t-test over the test set are displayed in Tab. 11. We observe that the improvement of all metrics is statistically significant under the significant level $\alpha = 0.05$, which demonstrates that our proposed LSTNet is conducive to the quality of the generated caption. Tab. 12 details the semantic subcategories of SPICE scores and p-values for t-test over the test set. We can observe that all semantic subcategories of SPICE are improved, which reveals the effectiveness and superiority of local visual modeling in LSTNet. Furthermore, we can also observe that under the significant level $\alpha = 0.05$, some semantic subcategories of SPICE (*i.e.*, Attribute, Size, Color, and Object) obtain significant improvements. Notably, all these four metrics describe the attributes of the object, so it proves that the local visual modeling in LSTNet is helpful to capture object-level information. Compared with other semantic metrics, the improvement of *Relation* metric is relatively insignificant. This may be because, to capture the relation between objects, it is not enough to only

Table 8: Ablation studies on LSA and LSF modules.

Module	B-1	B-4	M	R	C	S
w/o LSA+LSF	81.0	38.9	29.0	58.4	131.3	22.6
only LSA	81.2	39.7	29.3	59.1	133.6	22.8
only LSF	81.3	39.8	29.3	59.0	133.7	22.8
LSA + LSF	81.5	40.3	29.6	59.4	134.8	23.1

Table 9: Ablation studies on various fusion methods. All models are not equipped with LSA. FPN is the feature pyramid network similar to [47]. All values are reported as percentages (%), where B-N, M, R, C, and S are short for BLEU-N, METEOR, ROUGE-L, CIDEr, and SPICE scores.

Fusion methods	B-1	B-4	M	R	C	S
w/o Fuse	81.0	38.9	29.0	58.4	131.3	22.6
MLP	81.0	39.3	29.2	59.0	132.5	22.7
SumPool	81.1	39.4	29.1	59.0	132.5	22.7
3×3 Conv	81.3	39.7	29.0	58.9	132.6	22.7
FPN	81.1	39.1	29.1	58.7	132.6	22.6
LSF (ours)	81.3	39.8	29.3	59.0	133.7	22.8

improve the local modeling ability of the model and global modeling ability is also very important. For other semantic metrics of a single object (*i.e.*, Attribute, Size, Color, and Object), local visual modeling has been able to achieve significant performance improvement.

4.6. Qualitative Analysis

To qualitatively validate the effectiveness of LSTNet, we display several typical examples of captions generated by Transformer and LSTNet on the same grid features in Fig. 7. We can observe that the captions generated by Transformer are uninformative even erroneous, while the captions generated by LSTNet are more accurate and distinguishable, which demonstrates that our proposed LSA and LSF are helpful to recognize the visual object by local modeling.

To gain deep insights into the reason why LSTNet can generate accurate captions, we further illustrate the attention map of the top encoder layer in Transformer and LSTNet in Fig. 7. By analyzing the results, we gain the following observations: 1) The attention map produced by Transformer fails to attend to the important visual objects in the image, while LSTNet is able to focus on the important ones. For instance, for the image in the first

Table 10: Ablation studies on different grid sizes of the visual feature. All values are reported as percentages (%), where B-N, M, R, C and S are short for BLEU-N, METEOR, ROUGE-L, CIDEr, and SPICE scores.

Grid Size	B-1	B-4	M	R	C	S
1×1	78.5	36.2	27.4	56.5	120.3	20.6
2×2	79.9	37.7	28.3	57.7	124.9	21.7
3×3	80.4	38.9	28.8	58.4	129.6	22.3
4×4	80.6	38.9	28.9	58.5	130.3	22.4
5×5	81.0	39.6	29.1	58.8	131.7	22.7
6×6	81.3	39.9	29.3	58.9	132.1	22.9
7×7	81.5	40.3	29.6	59.4	134.8	23.1

Table 11: Performance comparisons of different captioning metrics for the Standard Transformer and our LSTNet. P-values come from two-tailed t-tests using paired samples. P-values in bold are significant at 0.05 significance level.

Model	BLEU-1	BLEU-4	METEOR	ROUGE	CIDEr	SPICE
Transformer	81.0	38.9	29.0	58.4	131.3	22.6
LSTNet	81.5	40.3	29.6	59.4	134.8	23.1
p-value	6.7×10^{-3}	3.3×10^{-7}	1.2×10^{-7}	8.0×10^{-7}	3.9×10^{-9}	1.2×10^{-4}

Table 12: Subcategories of SPICE metrics for the Standard Transformer and our proposed LSTNet. P-values are calculated by two-tailed t-tests using paired samples. Note that p-values in bold are significant at 0.05 significance level.

Model	SPICE					
	Relation	Cardinality	Attribute	Size	Color	Object
Transformer	6.91	20.58	11.80	4.71	12.93	40.35
LSTNet	7.06	22.68	12.38	4.84	14.60	40.76
p-value	0.298	0.059	0.002	0.048	0.001	0.009

Table 13: Comparison with state of the art on the Flickr8k dataset. All values are reported as percentages (%), where B-N, M, R, and C are short for BLEU-N, METEOR, ROUGE-L, and CIDEr scores. † indicates an ensemble model results.

Methods	B-1	B-4	M	R	C
Deep VS [40]	57.9	16.0	-	-	-
Google NIC [15]†	63.0	-	-	-	-
Soft-Attention [26]	67.0	19.5	18.9	-	-
Hard-Attention [26]	67.0	21.3	20.3	-	-
emb-gLSTM [48]	64.7	21.2	20.6	-	-
Log Bilinear [49]	65.6	17.7	17.3	-	-
LSTNet	67.4	24.3	21.5	44.8	63.6

row in Fig. 7, Transformer is focusing on the table and LSTNet is focusing on the man and phone. Thus, Transformer generates the erroneous caption (*i.e.*, “*tie*”, “*table*”), while LSTNet recognizes “*A man holding a cell phone*” correctly. 2) Transformer can only attend to one object or small area in the image, while LSTNet will focus on more primary objects, thus generating accurate and detailed descriptions. For example, for the images in the second row in Fig. 7, Transformer is only focusing on the mouth of the boy, and LSTNet is focusing on both the boy and the teddy bear. Thus, Transformer fails to recognize the “*teddy bear*” but only produces a general phrase (*i.e.*, “*a stuffed animal*”). Thanks to the precise attention in the encoder, LSTNet recognizes “*a young boy holding a teddy bear*” successfully. These observations reveal that our proposed LSA forces the model to focus on not only important but also comprehensive information in the image.

4.7. Attention Visualization

To better qualitatively evaluate the generated results with LSTNet, we visualize the contribution of each grid of the visual features during caption generation in Fig. 6. Technically, we average attention weights of 8 heads in the last decoder layer. We can observe that Transformer will attend to irrelevant regions, thus generating erroneous descriptions (*e.g.*, “*laptop*”). Instead, our proposed LSTNet can focus on correct grids when generating informative words like “*chair*” and “*umbrella*”. These observations demonstrate that our proposed LSA and LSF modules help the model consistently focus on the correct regions for image captioning by providing richer and

Table 14: Comparison with state of the art on the Flickr30k dataset. All values are reported as percentages (%), where B-N, M, R, and C are short for BLEU-N, METEOR, ROUGE-L and CIDEr scores. † indicates an ensemble model results.

Methods	B1	B4	M	R	C
Deep VS [40]	57.3	15.7	-	-	-
Google NIC [15]†	66.3	18.3	-	-	-
m-RNN [50]	60.0	19.0	-	-	-
Soft-Attention [26]	66.7	19.1	18.5	-	-
Hard-Attention [26]	66.9	19.9	18.5	-	-
emb-gLSTM [48]	64.6	20.6	17.9	-	-
ATT [51]†	64.7	23.0	18.9	-	-
Log Bilinear [49]	60.0	17.1	16.9	-	-
LSTNet	67.1	23.3	20.4	44.3	64.5

finer-grained visual features for the decoder through local interaction and fusion.

4.8. Generalization on the Flickr Datasets

To verify the generalization of our proposed LSTNet, we also conduct extensive experiments on the Flickr8k and Flickr30k datasets. The performance comparisons between our proposed LSTNet and previous SOTAs on Flickr8k [52] and Flickr30k [53] are shown in Tab 13 and Tab 14, respectively. As can be observed, our proposed LSTNet outperforms the previous SOTAs with a significant margin on both Flickr8k and Flickr30K. This verifies that our proposed LSTNet has strong generalization on other datasets.

5. Conclusion

In this paper, we propose LSTNet, a novel Locality-Sensitive Transformer Network for image captioning, which exploits the local interaction and fusion for better object recognition with grid features. Specifically, we design the LSA module to model the relationship within an encoder layer, which is helpful to attain the complete semantic information of each object and refine the details of visual features. We then introduce the LSF module to fuse visual features from different layers by modeling the relationships between adjacent grids, which leads to visual features with richer semantic information. Experimental results on the MS-COCO dataset demonstrate the significant

performance advantages of LSTNet over previous SOTA models. Extensive ablation studies and visualization comparisons further reveal the effectiveness and insights of the individual components of LSTNet. Additional experiments on the Flickr8k and Flickr30k datasets also verify the generalization of LSTNet on other datasets. Although the proposed LSTNet significantly improves the object location capability and the captioning performance, it also introduces additional computation and parameters. However, in comparison to the self-attention of the vanilla Transformer, the parameters and computation introduced by LSA and LSF modules are negligible.

References

- [1] M. Cornia, L. Baraldi, R. Cucchiara, Show, control and tell: A framework for generating controllable and grounded captions, in: Proceedings of the IEEE/CVF Conference on Computer Vision and Pattern Recognition, 2019, pp. 8307–8316.
- [2] M. Cornia, M. Stefanini, L. Baraldi, R. Cucchiara, Meshed-memory transformer for image captioning, in: Proceedings of the IEEE/CVF Conference on Computer Vision and Pattern Recognition, 2020, pp. 10578–10587.
- [3] T.-Y. Lin, M. Maire, S. Belongie, J. Hays, P. Perona, D. Ramanan, P. Dollár, C. L. Zitnick, Microsoft coco: Common objects in context, in: European conference on computer vision, 2014.
- [4] B. A. Plummer, L. Wang, C. M. Cervantes, J. C. Caicedo, J. Hockenmaier, S. Lazebnik, Flickr30k entities: Collecting region-to-phrase correspondences for richer image-to-sentence models, in: Proceedings of the IEEE international conference on computer vision, 2015, pp. 2641–2649.
- [5] P. Anderson, X. He, C. Buehler, D. Teney, M. Johnson, S. Gould, L. Zhang, Bottom-up and top-down attention for image captioning and visual question answering, in: Proceedings of the IEEE/CVF Conference on Computer Vision and Pattern Recognition, 2018, pp. 6077–6086.
- [6] S. Ren, K. He, R. Girshick, J. Sun, Faster r-cnn: towards real-time object detection with region proposal networks, *IEEE transactions on pattern analysis and machine intelligence* 39 (6) (2016) 1137–1149.

- [7] R. Krishna, Y. Zhu, O. Groth, J. Johnson, K. Hata, J. Kravitz, S. Chen, Y. Kalantidis, L.-J. Li, D. A. Shamma, et al., Visual genome: Connecting language and vision using crowdsourced dense image annotations, *IJCV* 123 (1) (2017) 32–73.
- [8] Y. Pan, T. Yao, Y. Li, T. Mei, X-linear attention networks for image captioning, in: *Proceedings of the IEEE/CVF Conference on Computer Vision and Pattern Recognition*, 2020, pp. 10971–10980.
- [9] L. Huang, W. Wang, J. Chen, X.-Y. Wei, Attention on attention for image captioning, in: *Proceedings of the IEEE international conference on computer vision*, 2019, pp. 4634–4643.
- [10] H. Jiang, I. Misra, M. Rohrbach, E. Learned-Miller, X. Chen, In defense of grid features for visual question answering, in: *Proceedings of the IEEE/CVF Conference on Computer Vision and Pattern Recognition*, 2020, pp. 10267–10276.
- [11] X. Zhang, X. Sun, Y. Luo, J. Ji, Y. Zhou, Y. Wu, F. Huang, R. Ji, Rst-net: Captioning with adaptive attention on visual and non-visual words, in: *Proceedings of the IEEE/CVF Conference on Computer Vision and Pattern Recognition*, 2021, pp. 15465–15474.
- [12] Y. Luo, J. Ji, X. Sun, L. Cao, Y. Wu, F. Huang, C.-W. Lin, R. Ji, Dual-level collaborative transformer for image captioning, in: *Proceedings of the AAAI Conference on Artificial Intelligence*, no. 3, 2021, pp. 2286–2293.
- [13] H. Wu, B. Xiao, N. Codella, M. Liu, X. Dai, L. Yuan, L. Zhang, Cvt: Introducing convolutions to vision transformers, *arXiv preprint arXiv:2103.15808* (2021).
- [14] V.-Q. Nguyen, M. Suganuma, T. Okatani, Grit: Faster and better image captioning transformer using dual visual features, in: *European Conference on Computer Vision*, Springer, 2022, pp. 167–184.
- [15] O. Vinyals, A. Toshev, S. Bengio, D. Erhan, Show and tell: A neural image caption generator, in: *Proceedings of the IEEE/CVF Conference on Computer Vision and Pattern Recognition*, 2015, pp. 3156–3164.

- [16] J. Lu, C. Xiong, D. Parikh, R. Socher, Knowing when to look: Adaptive attention via a visual sentinel for image captioning, in: Proceedings of the IEEE/CVF Conference on Computer Vision and Pattern Recognition, 2017, pp. 375–383.
- [17] J. Ji, Y. Ma, X. Sun, Y. Zhou, Y. Wu, R. Ji, Knowing what to learn: A metric-oriented focal mechanism for image captioning, *IEEE Transactions on Image Processing* (2022) 1–1doi:10.1109/TIP.2022.3183434.
- [18] Y. Ma, J. Ji, X. Sun, Y. Zhou, Y. Wu, F. Huang, R. Ji, Knowing what it is: Semantic-enhanced dual attention transformer, *IEEE Transactions on Multimedia* (2022) 1–1doi:10.1109/TMM.2022.3164787.
- [19] A. Vaswani, N. Shazeer, N. Parmar, J. Uszkoreit, L. Jones, A. N. Gomez, L. Kaiser, I. Polosukhin, Attention is all you need, *Advances in neural information processing systems* (2017).
- [20] C. Wang, Y. Shen, L. Ji, Geometry attention transformer with position-aware lstms for image captioning, *Expert Systems with Applications* 201 (2022) 117174. doi:https://doi.org/10.1016/j.eswa.2022.117174. URL <https://www.sciencedirect.com/science/article/pii/S0957417422005619>
- [21] Y. Wang, J. Xu, Y. Sun, A visual persistence model for image captioning, *Neurocomputing* 468 (2022) 48–59. doi:https://doi.org/10.1016/j.neucom.2021.10.014. URL <https://www.sciencedirect.com/science/article/pii/S0925231221014922>
- [22] Z. Zhang, Q. Wu, Y. Wang, F. Chen, Exploring pairwise relationships adaptively from linguistic context in image captioning, *IEEE Transactions on Multimedia* (2021).
- [23] X. Yang, Y. Liu, X. Wang, Reformer: The relational transformer for image captioning, in: Proceedings of the 30th ACM International Conference on Multimedia, 2022, pp. 5398–5406.
- [24] K. He, X. Zhang, S. Ren, J. Sun, Deep residual learning for image recognition, in: Proceedings of the IEEE/CVF Conference on Computer Vision and Pattern Recognition, 2016, pp. 770–778.

- [25] A. Rosenfeld, M. Thurston, Edge and curve detection for visual scene analysis, *IEEE Transactions on Computers* C-20 (5) (1971) 562–569. doi:10.1109/T-C.1971.223290.
- [26] K. Xu, J. Ba, R. Kiros, K. Cho, A. Courville, R. Salakhudinov, R. Zemel, Y. Bengio, Show, attend and tell: Neural image caption generation with visual attention, in: *International conference on machine learning*, PMLR, 2015, pp. 2048–2057.
- [27] O. Vinyals, A. Toshev, S. Bengio, D. Erhan, Show and tell: Lessons learned from the 2015 mscoco image captioning challenge, *IEEE transactions on pattern analysis and machine intelligence* 39 (4) (2016) 652–663.
- [28] Y. Ma, G. Xu, X. Sun, M. Yan, J. Zhang, R. Ji, X-clip: End-to-end multi-grained contrastive learning for video-text retrieval, in: *Proceedings of the 30th ACM International Conference on Multimedia*, 2022, pp. 638–647.
- [29] S. Ioffe, C. Szegedy, Batch normalization: Accelerating deep network training by reducing internal covariate shift, in: *International conference on machine learning*, PMLR, 2015, pp. 448–456.
- [30] X. Ding, X. Zhang, N. Ma, J. Han, G. Ding, J. Sun, Repvgg: Making vgg-style convnets great again, in: *Proceedings of the IEEE/CVF Conference on Computer Vision and Pattern Recognition*, 2021, pp. 13733–13742.
- [31] X. Ding, X. Zhang, J. Han, G. Ding, Diverse branch block: Building a convolution as an inception-like unit, in: *Proceedings of the IEEE/CVF Conference on Computer Vision and Pattern Recognition*, 2021, pp. 10886–10895.
- [32] S. J. Rennie, E. Marcheret, Y. Mroueh, J. Ross, V. Goel, Self-critical sequence training for image captioning, in: *Proceedings of the IEEE/CVF Conference on Computer Vision and Pattern Recognition*, 2017, pp. 7008–7024.
- [33] T. Yao, Y. Pan, Y. Li, Z. Qiu, T. Mei, Boosting image captioning with attributes, in: *Proceedings of the IEEE international conference on computer vision*, 2017, pp. 4894–4902.

- [34] W. Jiang, L. Ma, Y.-G. Jiang, W. Liu, T. Zhang, Recurrent fusion network for image captioning, in: European conference on computer vision, 2018, pp. 499–515.
- [35] T. Yao, Y. Pan, Y. Li, T. Mei, Exploring visual relationship for image captioning, in: European conference on computer vision, 2018.
- [36] X. Yang, K. Tang, H. Zhang, J. Cai, Auto-encoding scene graphs for image captioning, in: Proceedings of the IEEE/CVF Conference on Computer Vision and Pattern Recognition, 2019, pp. 10685–10694.
- [37] Z.-J. Zha, D. Liu, H. Zhang, Y. Zhang, F. Wu, Context-aware visual policy network for fine-grained image captioning, *IEEE Transactions on Pattern Analysis and Machine Intelligence* 44 (2) (2022) 710–722. doi:10.1109/TPAMI.2019.2909864.
- [38] G. Li, L. Zhu, P. Liu, Y. Yang, Entangled transformer for image captioning, in: Proceedings of the IEEE international conference on computer vision, 2019, pp. 8928–8937.
- [39] S. Herdade, A. Kappeler, K. Boakye, J. Soares, Image captioning: Transforming objects into words, *Advances in neural information processing systems* (2019).
- [40] A. Karpathy, L. Fei-Fei, Deep visual-semantic alignments for generating image descriptions, in: Proceedings of the IEEE conference on computer vision and pattern recognition, 2015, pp. 3128–3137.
- [41] K. Papineni, S. Roukos, T. Ward, W.-J. Zhu, Bleu: a method for automatic evaluation of machine translation, in: Proceedings of the 40th annual meeting of the Association for Computational Linguistics, 2002, pp. 311–318.
- [42] S. Banerjee, A. Lavie, Meteor: An automatic metric for mt evaluation with improved correlation with human judgments, in: Proceedings of the 40th annual meeting of the Association for Computational Linguistics, 2005, pp. 65–72.
- [43] C.-Y. Lin, Rouge: A package for automatic evaluation of summaries, in: Proceedings of the 40th annual meeting of the Association for Computational Linguistics, 2004, pp. 74–81.

- [44] R. Vedantam, C. Lawrence Zitnick, D. Parikh, Cider: Consensus-based image description evaluation, in: Proceedings of the IEEE/CVF Conference on Computer Vision and Pattern Recognition, 2015, pp. 4566–4575.
- [45] P. Anderson, B. Fernando, M. Johnson, S. Gould, Spice: Semantic propositional image caption evaluation, in: European conference on computer vision, Springer, 2016, pp. 382–398.
- [46] S. Xie, R. Girshick, P. Dollár, Z. Tu, K. He, Aggregated residual transformations for deep neural networks, in: Proceedings of the IEEE/CVF Conference on Computer Vision and Pattern Recognition, 2017, pp. 1492–1500.
- [47] S. Liu, L. Qi, H. Qin, J. Shi, J. Jia, Path aggregation network for instance segmentation, in: Proceedings of the IEEE/CVF Conference on Computer Vision and Pattern Recognition, 2018, pp. 8759–8768.
- [48] X. Jia, E. Gavves, B. Fernando, T. Tuytelaars, Guiding the long-short term memory model for image caption generation, in: Proceedings of the IEEE international conference on computer vision, 2015, pp. 2407–2415.
- [49] J. Donahue, L. Anne Hendricks, S. Guadarrama, M. Rohrbach, S. Venugopalan, K. Saenko, T. Darrell, Long-term recurrent convolutional networks for visual recognition and description, in: Proceedings of the IEEE conference on computer vision and pattern recognition, 2015, pp. 2625–2634.
- [50] J. Mao, W. Xu, Y. Yang, J. Wang, Z. Huang, A. Yuille, Deep captioning with multimodal recurrent neural networks (m-rnn), arXiv preprint arXiv:1412.6632 (2014).
- [51] Q. You, H. Jin, Z. Wang, C. Fang, J. Luo, Image captioning with semantic attention, in: Proceedings of the IEEE conference on computer vision and pattern recognition, 2016, pp. 4651–4659.
- [52] M. Hodosh, P. Young, J. Hockenmaier, Framing image description as a ranking task: Data, models and evaluation metrics, *Journal of Artificial Intelligence Research* 47 (2013) 853–899.
- [53] P. Young, A. Lai, M. Hodosh, J. Hockenmaier, From image descriptions to visual denotations: New similarity metrics for semantic inference over

event descriptions, *Transactions of the Association for Computational Linguistics* 2 (2014) 67–78.